AIAA 2002-3211

Effective Thermal Conductivity for Compact Heat Sink Models Based on the Churchill and Chu Correlation

Kyle A. Brucker, Kyle Ressler and Joseph Majdalani
Marquette University
Milwaukee, WI 53233

8th AIAA/ASME Joint Thermophysics and Heat Transfer Conference
24–26 June 2002
St. Louis, MO

Effective Thermal Conductivity for Compact Heat Sink Models Based on the Churchill and Chu Correlation

Kyle A. Brucker,* Kyle Ressler,† and Joseph Majdalani‡
Marquette University, Milwaukee, WI 53233

In this study an asymptotic technique is presented for calculating the equivalent thermal conductivity of a compact heat sink model. The method uses the known Nusselt number correlation given by Churchill and Chu for both laminar and turbulent regimes. This correlation is valid for airflow over a vertical flat plate and is applicable over the entire range of Rayleigh and Prandtl numbers. The resulting asymptotic solution presented here is applicable for overall heat transfer coefficients ranging from 0 to 100,000 $\mathrm{Wm^{-2}K^{-1}}$. The closed-form analytical solution is compared to an iterative numerical solution and found to exhibit a very small error over a wide range of flow conditions. Being practically equivalent to the numerical solution, the asymptotic correlation obviates the need for guesswork and iteration in a compact heat sink simulation. It enables the implementation of a self-contained numerical scheme that does not require user intervention.

Nomenclature

A = $\left(\mathrm{Gr}_L\, \mu C_P\right)^{1/6} = \left(g\beta\, \Delta T L^3 \rho^2 C_p / \mu\right)^{1/6}$
C_p = constant pressure specific heat
g = acceleration due to gravity
Gr_L = Grashof number, $g\beta\, \Delta T L^3 \rho^2 \mu^{-2}$
h_e = effective heat transfer coefficient
k_e = effective thermal conductivity
L = characteristic length
Pr = Prandtl number, $\mu C_p / k_e$
Ra = Rayleigh number, $g\beta \Delta T L^3 \rho^2 \mu^{-2}\mathrm{Pr}$
T_s = maximum surface temperature
T_∞ = ambient air temperature
T_f = film temperature, $(T_s + T_\infty)/2$
U = overall heat transfer coefficient, $\dot{Q}/\left(A\Delta T\right)$

β = thermal expansion coefficient, $1/T_f$
ΔT = $T_S - T_\infty$
μ = viscosity of air at T_f
ρ = density of air at T_f

*Graduate Research Assistant. Presently at Cornell University, Ithaca, NY. Member AIAA.
†Graduate Research Assistant. Presently at Washington University in St. Louis, Saint Louis, MO. Member AIAA.
‡Assistant Professor, Department of Mechanical and Industrial Engineering. Member AIAA.

I. Introduction

THE electronic devices of today and possibly of the near future are bound to rely on integrated circuit chips and printed circuit boards. The increasingly more stringent demand for these components to be both smaller and faster is not without pitfall. Clearly, the compounding effects of size reduction and increased power lead to higher heat generation per unit area. So far one of the most popular methods for dissipating the constantly escalating heat fluxes has been accomplished through the use of heat sinks.

The current literature is filled with examples of where heat sinks have been effectively used. In Azar *et al.*,[1] design optimization of ducted heat sinks is considered. This optimization is based on correlations that relate fin thickness and duct spacing. In Knight *et al.*[2,3] a method to optimize heat sinks is proposed whereby the number of closed-finned ducts is varied under force convection conditions. In Sasaki and Kishimoto,[4] a method is suggested to determine the optimal heat sink dimensions of water-cooled heat sinks given a specified pressure drop. A more detailed account of studies concerned with design optimization and selection can be found in Lee[5] and Patel and Belady.[6] These studies have several aspects in common, including their reliance on standard heat transfer correlations[6] for calculating thermal characteristics.

Although this method of heat removal is highly effective in practice, it can be computationally demanding during layout design stages. The main problem is not as much with the modeling of one heat sink as it is with coupled arrays of multiple cooling elements. Since the performance of each sink is dependent on the temperature difference between the surrounding fluid and its surface temperature, analyzing several adjacent sinks independently of their surrounding thermofluid conditions is both impractical and prone to error. Moreover, numerical models of coupled heat sinks often lead to a computationally intensive problem requiring large memory resources and CPU time. In many applications, the computational cost poses unrealistic barriers between board design and thermal analysis. This is especially true during the design and construction of arrays comprising multiple heat sinks separated by small characteristic distances. Although the possibility exists for discretizing the multi-component layout with sufficiently fine grids, the iterative solution of resulting meshes can lead to significant delays during the integrated design and verification stages. For this reason, conventional methods based on large-scale discretization of actual heat sinks are often viewed as inadequate in handling large numbers of cooling components. The search for a feasible alternative has led many researchers to employ a lumped approach in representing a given heat sink. This is exemplified by the use of compact heat sink models that have become ever so popular in the electronic cooling community. Their popularity, one can argue, may be attributed to their ability to cut down feedback time between designers and thermal analysts while providing fast and reliable predictions.

The compact heat sink idea is based on the principle that a heat sink may be replaced by a 'volumetric fluid block' exhibiting the same effective thermal conductivity and flow resistance as those of the actual cooling element. The idea of using a fluid block as a substitute for the actual heat sink has been successfully introduced in forced convection applications by Patel and Belady.[6] In natural convection studies, it has been recently applied by Narasimhan and Majdalani.[7,8]

It should be noted that Patel and Belady's expedient approach distributes the heat produced by the microchip uniformly over the heat sink volume. This operation permits the heating mechanism of the airstream to be accounted for. During this process, CFD modeling is used to estimate the relevant air temperatures that are needed to calculate the base temperature of the heat sink. The technique becomes iterative only when considering a different heat sink design.

An alternative procedure based on the 'extended flat plate model' has also been employed by Culham, Lee and Yovanovich.[9] Culham's flat plate boundary layer model offers a simple and straightforward method for calculating the equivalent thermal performance of rectangular heat sinks. This is accomplished through the use of an extended surface area exhibiting a lower thermal resistance between the base plate and cooling fluid. Despite their dissimilarities, the two approaches lead to simpler thermal representations.

In the fluidic block model, the enhanced thermal character is not assigned to the base plate but, rather, to the volume of fluid representing the actual heat sink. Instead of increasing the base plate's convection heat transfer coefficient (to account for the absence of fin area), the thermal conductivity of the volumetric block above the base plate is increased. This is done in an effort to reproduce a temperature map that is closer to reality. This approach can be advantageous since the temperature field produced in microelectronic packages can be extremely complex due to the conjugate interaction between the cooling fluid and the various components of PCB packages. In essence, this is implemented by increasing the overall heat transfer coefficient between the base plate and the cooling fluid. To do so one must change the thermal property of the fluidic block above the base plate in a manner to reproduce the same overall thermal resistance associated with the actual heat sink. Using the same cooling fluid (say air), the problem becomes that of finding the specific thermal conductivity that must be assigned to the modified fluid in order to ensure the equivalence of actual and compact systems.

The validity of using standard Nusselt number correlations to evaluate the effective thermal conductivity is discussed at length by Narasimhan and Majdalani.[7,8] In these studies, a less than 5% error is incurred between detailed and compact models of numerically simulated extruded and pin-fin heat sinks. The small error in the compact models is absorbed at the benefit of cutting down time-to-convergence by a factor of 10. This example confirms the usefulness of compact models in providing significant time savings in comparison to direct simulations. Nonetheless, these compact models are by no means fully optimized themselves. As indicated by Narasimhan and

Majdalani,[7,8] one of the challenges in devising a compact model stands in the need for the iterative determination of the equivalent thermal conductivity from transcendental Nusselt number correlations.

Consider, for example, one of the most widely used correlations that is applicable over the entire range of Grashof numbers. As proposed by Churchill and Chu,[10] this correlation has the known form

$$\mathrm{Nu}_L = UL/k_e = h_e L/k_e = \left\{a_0 + a_1 \mathrm{Ra}^{1/6}\left[1+(a_3/\mathrm{Pr})^{9/16}\right]^{-8/27}\right\}^2 \qquad (1)$$

where $a_0 = 0.825$, $a_1 = 0.387$ and $a_2 = 0.492$. Note that U is used here instead of the effective heat transfer coefficient of the actual heat sink h_e to reflect the fact that radiation is often accounted for while determining the overall thermal resistance of a given heat sink.[7,8] According to Bejan,[11] Eq. (1) is expected to hold for $10^{-1} < \mathrm{Gr}_L < 10^{12}$ and for all Prandtl numbers (cf. pp. 192-193). The complexity, however, stems from the thermal conductivity k_e being simultaneously present in the expressions for the Nusselt, Rayleigh, and Prandlt numbers. Direct algebraic extraction of k_e is therefore impossible due to the several fractional powers. At present, this equation is solved iteratively for the equivalent thermal conductivity. In fact, the iterative scheme used in former studies requires user-intervention to provide initial guesses and selection of the meaningful root emerging from Eq. (1). Undoubtedly, a direct solution for k_e would provide additional CPU-savings by reducing the total number of computational cycles in a full-scale simulation of multiple arrays. This is especially true since all parameters in Eq. (1) except k_e are known a priori.[7,8] For this reason, it is the purpose of this note to show that k_e can be determined explicitly through the use of asymptotic perturbation tools. The resulting root will be shown to be sufficiently accurate; especially considering that Eq. (1) is given with a ±25% margin for error. The advantage of a closed-form solution for k_e will be the preclusion of guesswork and user-intervention in a compact heat sink simulation.

Before proceeding with the asymptotic analysis, it may be useful to note that the thermal conductivity solved for is not that of the cooling fluid. Rather, it is the equivalent thermal conductivity of the lumped fluidic block that replaces the heat sink above the base plate (see Fig. 1). This increased thermal conductivity mimics the effect of extended fins in improving the overall heat transfer coefficient from the base plate to the surroundings.[7,8]

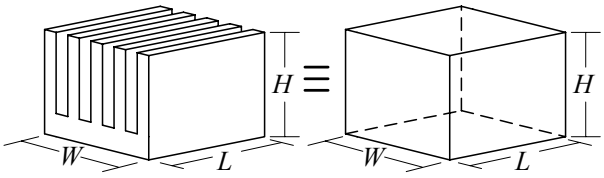

Fig. 1 Schematic of a detailed (flat plate) heat sink and the equivalent volumetric block of fluid whose increased thermal conductivity k_e gives the compact model the same thermal resistance as that of the detailed heat sink.

II. Direct Solution for Thermal Conductivity

The detailed derivation of the solution for the equivalent thermal conductivity is based on the theory of asymptotic analysis. This process requires expanding the transcendental equation for k_e into a binomial-type series of progressively diminishing terms. The resulting asymptotic series is then truncated by retaining only the first few terms needed to achieve a given level of precision. Due to the form of the Nusselt number correlation, one obtains a series in k_e, namely, $UL = R_0 k_e^{r_0} + R_1 k_e^{r_1} + R_2 k_e^{r_2} \ldots$ where R_i and r_i are pure constants. While R_i is related to the fluid properties and boundary conditions, r_i is a fractional exponent stemming from the binomial expansion. Due to the presence of the universal Prandtl number function in Eq. (1), two different binomial expansions will be possible depending on the size of k_e. This will generally lead to two separate solutions which become increasingly more accurate when k_e is either small or large, respectively. Each expansion will hence be valid only over a given range of the solution domain. Nonetheless, by retaining sufficient terms in each series, a uniformly valid solution can be arrived at over the entire range of interest.

For each of the two possible series expansions in k_e, the approach for finding a direct solution follows fundamental asymptotic guidelines. The term with the largest influence is first identified and retained as the leading or zeroth-order solution. This involves balancing the dominant terms in the resulting expansion. The zeroth-order approximation is then written as $k_e \cong k_0$. The next step is to substitute $k_e \cong k_0 + k_1 + \ldots$; where $k_1 \ll k_0$, back into the original expansion. Naturally, terms involved in the construction of k_0 will cancel so that a direct solution for k_1 may be

realized by balancing the second largest term that could not be accounted for in k_0. In like fashion, the process is repeated until a sufficient degree of precision is obtained. The details of these operations are described next.

Starting with Eq. (1), a binomial expansion is used to remove the squared exponent applied to the outer braces. This enables us to write

$$UL/k_e = a_0{}^2 + 2\times a_0 \times a_1 \mathrm{Ra}^{1/6}\left[1+(a_2/\mathrm{Pr})^{9/16}\right]^{-8/27} + \left\{a_1 \mathrm{Ra}^{1/6}\left[1+(a_2/\mathrm{Pr})^{9/16}\right]^{-8/27}\right\}^2 \quad (2)$$

For simplicity, we find it convenient to define

$$A=\left[g\beta\left(T_s-T_\infty\right)L^3\rho^2 C_p/\mu\right]^{1/6} \quad (3)$$

and then substitute A into Eq. (2). Putting $\mathrm{Pr}=\mu C_p/k_e$ and multiplying through by k_e, the following expression is obtained:

$$UL = a_0{}^2 k_e + 2a_0 a_1 k_e^{5/6} A\left[1+\left(\frac{a_2 k_e}{\mu C_P}\right)^{9/16}\right]^{-8/27} + a_1{}^2 k_e{}^{2/3} A^2\left[1+\left(\frac{a_2 k_e}{\mu C_P}\right)^{9/16}\right]^{-16/27} \quad (4)$$

In Eq. (4) a solution for k_e is still complicated by the presence of $[1+f(k_e)]^\alpha$ terms in brackets. Noting that $f\left(k_e\right)=[a_2 k_e/(\mu C_p)]^{9/16}$, Eq. (4) can be either divergent or convergent depending on the size of k_e. To ensure convergence, two solutions will have to be constructed for small and large k_e. In what follows, these solutions will be labeled type I and II, respectively.

A. Type-I Solution for Small U

To ensure convergence to the desired solution, we first let

$$w=\left[a_2 k_e/(\mu C_p)\right]^{9/16} \quad (5)$$

and then expand the two $[1+f(k_e)]^\alpha$ terms arising in Eq. (4). Using the binomial formula, one may put

$$T_1 = 1-\tfrac{8}{27}w+\tfrac{140}{729}w^2+\ldots,\ T_2 = 1-\tfrac{16}{27}w+\tfrac{344}{729}w^2+\ldots \quad (6)$$

which, when substituted into Eq. (4), give

$$UL = a_0 k_e + 2a_0 a_1 A k_e^{5/6} T_1 + a_1{}^2 A^2 k_e^{2/3} T_2 \quad (7)$$

At this point, the powers of k_e need to be exposed by inserting Eq. (6) into Eq. (7). One gets

$$UL = a_0{}^2 k_e + 2a_0 a_1 A\left(k_e^{5/6} - \tfrac{8}{27}uk_e^{67/48} + \tfrac{140}{729}u^2 k_e^{47/24}\right) + a_1{}^2 A^2\left(k_e^{2/3} - \tfrac{16}{27}uk_e^{59/48} + \tfrac{344}{729}u^2 k_e^{43/24}\right) \quad (8)$$

where $u\equiv(a_2/\mu C_P)^{9/16}$. The next step is to determine which term has the most impact on the solution. In determining which term has the largest impact on the solution, all negative terms must be eliminated because k_e is strictly positive. Contributions due to negative terms must be accounted for at the subsequent approximation level. The five terms that are left to be considered are:

$$UL = a_0{}^2 k_e + 2a_0 a_1 A k_e^{5/6} + \tfrac{280}{729}a_0 a_1 A u^2 k_e^{47/24} + a_1{}^2 A^2 k_e^{2/3} + \tfrac{344}{729}a_1{}^2 A^2 u^2 k_e^{43/24} \quad (9)$$

The candidates for leading-order terms are obtained by equating the left-hand side of Eq. (9) by one of the remaining positive terms before solving for k_e. These quantities are then labeled in the order in which they appear and then plotted in Fig. 2 alongside the numerical solution for k_e. As one may infer from the graph, while terms 1 and 2 lead to an over-prediction, terms 3 and 5 under-predict k_e. Term 4, on the other hand, matches the numerical solution very well for $U<10\ \mathrm{Wm^{-2}K^{-1}}$. Using the superscript to indicate the solution type, we thus identify the zeroth-order term of the solution to be $k_0^{\mathrm{I}}\equiv[UL/(a_1{}^2A^2)]^{3/2}$, where the superscript denotes the solution type. To find the next correction in the perturbation series, we then put

$$k_e^{\mathrm{I}} = \left[UL/(a_1{}^2A^2)\right]^{3/2} + k_1^{\mathrm{I}} \quad (10)$$

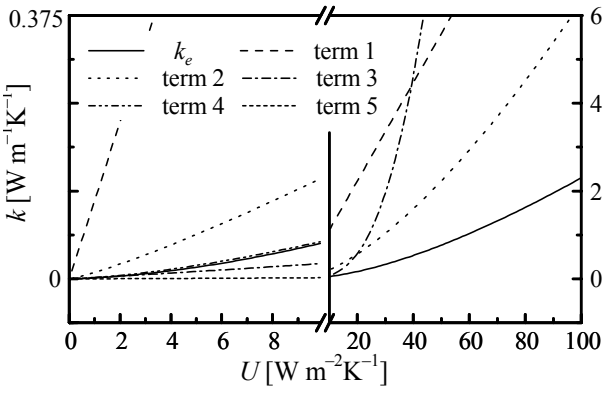

Fig. 2 Order of magnitude comparison based on different terms arising in the expansion of Churchill and Chu's Nusselt number correlation. Note that while term 4 dominates for small *U*, all three terms 1, 2, and 3 are needed to find the leading order behavior of the large *U* solution.

and substitute back into Eq. (8). After some algebra, we get

$$k_1^{\mathrm{I}} = -\tfrac{3}{2}\Big\{a_0^2 (k_0^{\mathrm{I}})^2 + 2a_0 a_1 A\Big[(k_0^{\mathrm{I}})^{11/6} - \tfrac{8}{27}u(k_0^{\mathrm{I}})^{115/48} + \tfrac{140}{729}u^2 (k_0^{\mathrm{I}})^{71/24}\Big] + a_1^2 A^2 u\Big[\tfrac{344}{729}u(k_0^{\mathrm{I}})^{67/24} - \tfrac{16}{27}(k_0^{\mathrm{I}})^{107/48}\Big]\Big\}/(UL) \tag{11}$$

To find higher-order correction terms, one may repeat the process to generate a recurrence relation. One finds, for $n = 2, 3, \ldots$, the following general form:

$$k_n^{\mathrm{I}} = -\tfrac{3}{2}k_0^{\mathrm{I}} k_{n-1}^{\mathrm{I}}\Big\{a_0^2 + a_0 a_1 A\Big[\tfrac{5}{3}(k_0^{\mathrm{I}})^{-1/6} - \tfrac{67}{81}u(k_0^{\mathrm{I}})^{19/48} + \tfrac{1645}{2187}u^2 (k_0^{\mathrm{I}})^{23/24}\Big] + a_1^2 A^2 u\Big[\tfrac{1849}{2187}u(k_0^{\mathrm{I}})^{19/24} - \tfrac{59}{81}(k_0^{\mathrm{I}})^{11/48}\Big]\Big\}/(UL) \tag{12}$$

Nonetheless, using the characteristic constants of the Churchill and Chu correlation, one may verify that a two-term approximation is adequate for all practical purposes.

B. Type-II Solution for Large U

In this case, the two $[1+f(k_e)]^{\alpha}$ terms in Eq. (4) must be written as $[f(k_e)]^{\alpha}[1+1/f(k_e)]^{\alpha}$ and then expanded. This turns Eq. (4) into

$$UL = a_0^2 k_e + 2a_0 a_1 A u^{-8/27} k_e^{2/3} + a_1^2 A^2 u^{-16/27} k_e^{1/3} - \tfrac{16}{27}a_1^2 A^2 u^{-43/27} k_e^{-11/48} \tag{13}$$

Terms that are not shown have an insignificant contribution. In fact, we find that the first three terms on the right-hand side together dominate the leading-order behavior. The fourth term is found to be small, but not so small that it can be ignored. Being both negative and inversely proportional to k_e, the fourth term cannot be a candidate for a leading-order solution. For this reason, only the first three terms are plotted in Fig. 2 in the large U range. As shown in the graph, not one single term dominates by itself. In seeking the leading-order solution, we therefore include all except the last term in Eq. (13). The problem becomes that of solving for the real root of the cubic polynomial emerging from

$$-c_1 + c_2 k_e^{1/3} + c_3 k_e^{2/3} + c_4 k_e = 0\,; \tag{14}$$

where

$$c_1 = UL\,,\quad c_2 = a_1^2 A^2 u^{-16/27}\,,\ c_3 = 2a_0 a_1 A u^{-8/27}\,,\ c_4 = a_0^2 \tag{15}$$

The corresponding root may be exacted from

$$k_0^{\mathrm{II}} = \left(c_1 - c_3 p_1^2 - c_2 p_2\right)/c_4 \tag{16}$$

where

$$p_1 \equiv \tfrac{1}{6}(36c_2c_3c_4 + 108c_1c_4^2 - 8c_3^3 + p_2)^{1/3}/c_4 - \tfrac{2}{3}(3c_2c_4 - c_3^2)/[c_4(36c_2c_3c_4 + 108c_1c_4^2 - 8c_3^3 + p_2)^{1/3}] - \tfrac{1}{3}(c_3/c_4) \tag{17}$$

$$p_2 \equiv 12\sqrt{3}c_4(27c_1^2c_4^2 - c_2^2c_3^2 - 4c_1c_3^3 + 4c_2^3c_4 + 18c_1c_2c_3c_4)^{1/2} \tag{18}$$

In order to account for the small correction associated with the fourth term in Eq. (13), we also try setting

$$k_e^{\mathrm{II}} = k_0^{\mathrm{II}} + k_1^{\mathrm{II}} \tag{19}$$

and substitute back into the expanded Churchill and Chu correlation. A linear corrective term can then be used to estimate the contribution that the additional $-\tfrac{16}{27}a_1^2 A^2 u^{-43/27} k_e^{-11/48}$ term would have on the solution. One finds

$$k_1^{\mathrm{II}} = -\left(\tfrac{16}{27}a_1^2 A^2 (k_0^{\mathrm{II}})^{-11/48} u^{-43/27}\right)/\left(a_0^2 + \tfrac{1}{3}a_1^2 A^2 \times (k_0^{\mathrm{II}})^{-2/3} u^{-16/27} + \tfrac{4}{3}a_0 a_1 A (k_0^{\mathrm{II}})^{-1/3} u^{-8/27}\right) \tag{20}$$

This two-term approximation is accurate to the point of obviating the need for higher-order corrections.

C. Solution for All U

It should be noted that the asymptotic errors in k_e^{I} and k_e^{II} increase as $U \to \infty$ and $U \to 0$, respectively. However, there exists a critical point U^* for which the relative error is the same in both approximations. This critical case occurs at the point for which the discrepancies between asymptotics and numerics become equal to the maximum error in each approximation. Mathematically, the critical condition corresponds to

$$\left|k_e - k_e^{\mathrm{I}}\right| = \left|k_e - k_e^{\mathrm{II}}\right| \tag{21}$$

By solving Eq. (21) for U^*, one is able to express the solution for the effective thermal conductivity over the entire physical range, namely, by setting

$$k_e = \begin{cases} k_e^{\mathrm{I}}; & 0 \le U \le U^* \\ k_e^{\mathrm{II}}; & U > U^* \end{cases} \tag{22}$$

For clarity, one may insert Churchill and Chu's constants into Eq. (16) and (20) to evaluate the first two terms of Eq. (22). One obtains, for the small U case,

$$k_e^{\mathrm{I}} = 17.25A^{-3}(UL)^{3/2} + k_1^{\mathrm{I}} \tag{23}$$

$$\begin{aligned} k_1^{\mathrm{I}} = -[&1.021(k_0^{\mathrm{I}})^2 + 0.957A(k_0^{\mathrm{I}})^{11/6} - 0.284Au(k_0^{\mathrm{I}})^{115/48} \\ &+0.184Au^2(k_0^{\mathrm{I}})^{71/24} - 0.133A^2u(k_0^{\mathrm{I}})^{107/48} \\ &+0.106A^2u^2(k_0^{\mathrm{I}})^{67/24}]/(UL) \end{aligned} \tag{24}$$

$$\begin{aligned} k_n^{\mathrm{I}} = -k_0^{\mathrm{I}}k_{n-1}^{\mathrm{I}}[&1.021 + 0.789A(k_0^{\mathrm{I}})^{-1/6} - 0.396Au(k_0^{\mathrm{I}})^{19/48} \\ &+0.360Au^2(k_0^{\mathrm{I}})^{23/24} - 0.164A^2(k_0^{\mathrm{I}})^{11/48}u \\ &+0.189A^2u^2(k_0^{\mathrm{I}})^{19/24}]/(UL) \end{aligned} \tag{25}$$

and, for the large U case,

$$\begin{aligned} k_0^{\mathrm{II}} &= 1.47UL - 1.056Av^{1/6} \\ &\times(0.2449z + 0.1265Av^{1/3}/z - 0.352Av^{1/6})^2 \\ &-0.2787A^2v^{1/3}(0.2449z + 0.1265A^2v^{1/3}/z - 0.352Av^{1/6}) \end{aligned} \tag{26}$$

where

$$v \equiv \mu C_P$$

$$z \equiv \left(\begin{matrix} 0.3712A^3v^{1/2} + 50.03UL \\ +6.094\sqrt{ULA^3v^{1/2} + 67.4U^2L^2} \end{matrix} \right)^{1/3}; \tag{27}$$

and

$$\begin{aligned} k_1^{\mathrm{II}} = A^2v^{43/48}(k_0^{\mathrm{II}})^{-11/48}/[&4.062 + 0.377A^2v^{1/3}(k_0^{\mathrm{II}})^{-2/3} \\ &+2.859Av^{1/6}(k_0^{\mathrm{II}})^{-1/3}] \end{aligned} \tag{28}$$

III. Comparison with Numerics

By way of verification, Eq. (22) is compared in Fig. 3 to the iterative solution for four different sets of flow and heat sink configurations. The operating parameters used in these test cases are listed in Table 1. Note that two of the four cases correspond to actual heat sinks described in previous studies.[7,8] It can be seen from these plots that Eq. (22) leads to a good agreement with the numerical solution over a wide range of overall heat transfer coefficients. In fact, an examination of the error behavior associated with these approximations is provided in Fig. 4 where both absolute and relative errors are graphed versus U alongside k_e.

From Fig. 4, it can be seen that the absolute error is very small everywhere. While the absolute error increases with U and the case number (or L), the relative error diminishes with both. However, the

Table 1 Sample test cases

Case	L	ρ	μ	C_p	T_s	T_∞
	m	$\mathrm{kgm^{-3}}$	$\mathrm{kgm^{-1}s^{-1}}$	$\mathrm{Jkg^{-1}K^{-1}}$	K	K
1	0.01500	1.078	1.982E-05	1007	361.4	293.15
2*	0.03048	1.091	1.965E-05	1007	354.0	293.15
3*	0.07620	1.103	1.949E-05	1007	346.6	293.15
4	0.15000	1.116	1.932E-05	1007	339.2	293.15

*Commercial heat sinks used by Narasimhan and Majdalani.[7,8]

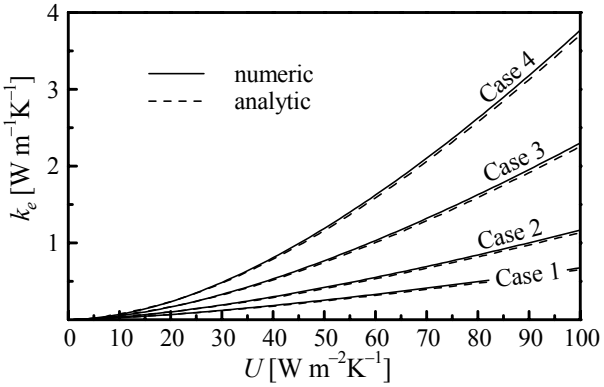

Fig. 3 Comparison between analytic and numeric solutions for the four cases given in Table 1 over the range $0 \le U \le 100$ Wm^{-2}K^{-1}.

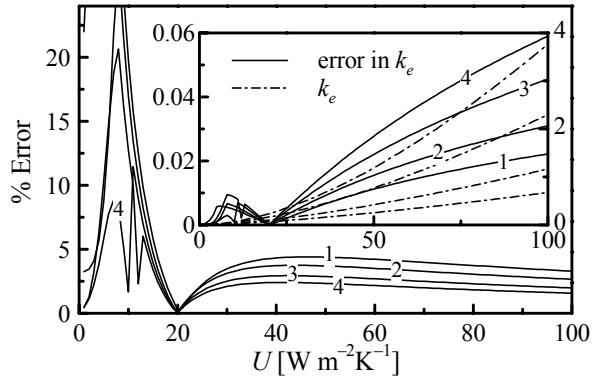

Fig. 4 Absolute and relative errors in the four test cases over the range $0 \le U \le 100$ Wm^{-2}K^{-1}. Note that the relative asymptotic error is large in a narrow region separating the small and large U approximations of k_e.

relative error rises in the $5 < U < 15$ range where k_e is small. In this 'buffer' region, the maximum relative error in each approximation is realized, specifically, at $U = U^*$. This critical line along which the error in both approximations is largest is plotted in Fig. 5 as a function of the surface temperature T_s and the characteristic length in the streamwise direction L. This plot is important because it provides the delineation line separating the small and large U approximations.

In order to allow for a self-contained algorithm, the data in Fig. 5 can be expressed in the form of $U^* = f(T_s, L)$. Although U^* is consulted only once for a given application range (i.e., to ensure that the type-I or type-II solutions are needed), it is helpful to express U^* in closed form. Using the method of least-squares for sigmoidal functions, one obtains:

$$U^* = \frac{A_1 - A_2}{1 + (L/L_0)^p} + A_2;$$

$$\begin{cases} A_1 = -10.799 + 12.352 e^{-T_s/57.37} \\ A_2 = 9.916 + 0.016 T_s + 0.000395 T_s^2 \\ L_0 = 0.0189 + 0.0516 e^{-T_s/30.258} \\ p = 0.586 + 0.15 e^{-T_s/33.606} \end{cases} \qquad (29)$$

Equation (29) reproduces the data in Fig. 5 to within ±2%.

Also given in Fig. 5 is the magnitude of the maximum relative error. Clearly, the latter appears to be less sensitive to the temperature difference between the base plate and the cooling fluid. We find that, for $L \geq 0.04$ m, the maximum relative error is smaller than 23.6% over the entire range of U irrespective of T_s. We conclude that, regardless of L or T_s, our asymptotic expressions represent reasonably accurate representations of the Churchill and Chu relation, especially that the asymptotic error drops very quickly when operating away from the critical $U = U^*$ line.

Generally, for problems characterized by overall heat transfer coefficients in excess of 20, it is safe to use k_e^{II} to obtain suitable predictions. Using Case 3 as an example, one may fix the length and allow the overall heat transfer coefficient to vary. When this is accomplished, the relative error starts at 0.45% at $U = 1$, increases to 11.4% at $U = 11$, drops to 3% at $U = 40$, then again to 2% at $U = 100\,\mathrm{Wm^{-2}K^{-1}}$. Further out, the error continues to decrease as $U \to \infty$.

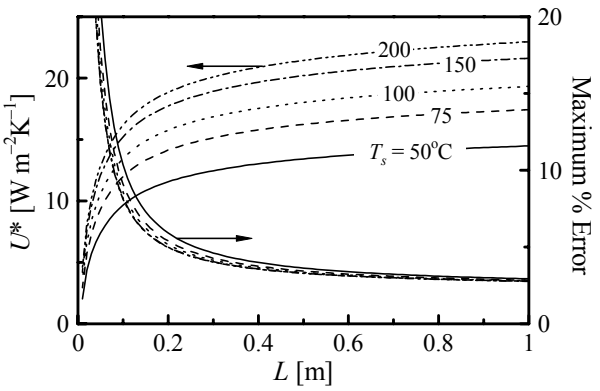

Fig. 5 Critical lines producing the maximum asymptotic error as function of the characteristic length in the streamwise direction. Results correspond to the cooling fluid being air at $T_\infty = 20^{\circ}\mathrm{C}$.

Thus, although most figures stop at $U = 100\,\mathrm{Wm^{-2}K^{-1}}$, the mathematical validity of Eq. (22) continues to improve with successive increases in U.

For the extruded-fin heat sink considered by Narasimhan and Majdalani,[7,8] the base plate has dimensions of $0.0762\,\mathrm{m} \times 0.0412\,\mathrm{m}$ and dissipates 8 watts according to the temperature distribution prescribed in Table 1 for Case 3. A detailed numerical simulation of the entire heat sink yields $U = 47.73\,\mathrm{Wm^{-2}K^{-1}}$, wherefrom an effective thermal conductivity of $k_e = 0.712\,\mathrm{Wm^{-1}K^{-1}}$ is deduced. The asymptotic solution given by Eq. (22) yields a close value of $0.70\,\mathrm{Wm^{-1}K^{-1}}$. This small error in the analytic prediction is easily justifiable, being merely 4.2% in disagreement with the experimental value of $0.721\,\mathrm{Wm^{-1}K^{-1}}$ reported by Kusha, Rosenblat, and Lee.[12]

IV. Practical Implementation

Having developed a closed-form solution for the effective thermal conductivity, its actual implementation can be illustrated through an example corresponding to the heat sink analyzed experimentally by Kusha, Rosenblat, and Lee.[13] The same heat-sink configuration has been computationally modeled by Narasimhan and Majdalani,[7,8] the details of which are listed as Case 3 in Table 1.

To determine the equivalent thermal conductivity of the compact model, one must specify $U, L, \rho, \mu, T_s, T_\infty, g$ and C_p. Based on $L = 0.0762\,\mathrm{m}$ and $T_s = 346.6\,\mathrm{K}$, one evaluates the critical $U^* = 10\,\mathrm{Wm^{-2}K^{-1}}$ (from Fig. 5 or Eq. (29)). Since

$U = 47.73\ \mathrm{Wm^{-2}K^{-1}}$ exceeds U^*, the application at hand requires the use of the type-II solution for k_e.

Based on the Eqs. (3) and (26)-(28), one can immediately program and determine:

$$\begin{cases} A = 5.978\,(\mathrm{Wm^{-1}K^{-1}})^{1/6} \\ v = 0.0196\ \mathrm{Wm^{-1}K^{-1}} \\ z = 7.279\,(\mathrm{Wm^{-1}K^{-1}})^{1/3} \\ k_0^{\mathrm{II}} = 0.6340\ \mathrm{Wm^{-1}K^{-1}} \\ k_1^{\mathrm{II}} = 0.0606\ \mathrm{Wm^{-1}K^{-1}} \end{cases}, \qquad (30)$$

and so,

$$k_e = k_0^{\mathrm{II}} + k_1^{\mathrm{II}} = 0.70\ \mathrm{Wm^{-1}K^{-1}}. \qquad (31)$$

This value is then used to define the thermal resistance of the compact model needed in the CFD simulation. These steps are illustrated by the flowchart of Fig. 6 which pertains to both small and large $-U$ applications.

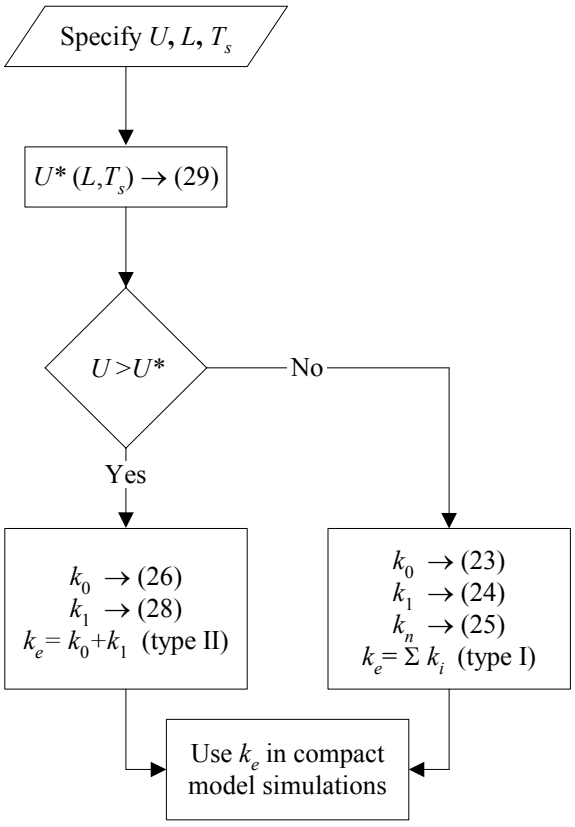

Fig. 6 Flowchart describing the simple steps leading to the direct determination of k_e for a compact model simulation of an actual heat sink.

V. Concluding Remarks

In this study, a piecewise solution is obtained for the effective thermal conductivity of a compact heat sink model over the entire range of Grashof and Prandtl numbers ($10^{-1} < \mathrm{Gr}_L < 10^{12}$, $\forall\,\mathrm{Pr}$, $\forall U$, and $\forall T_s$). The lumped thermal approach is particularly relevant to the development of simplified models of parallel-plate and pin-fin heat sinks. Aside from the technical merit in providing quick and direct estimations of k_e, the asymptotic methodology introduced here can be useful in overcoming the transcendental character encountered in other heat transfer relations similar to the Churchill and Chu correlation. From a practical standpoint, the availability of a closed-form expression enables thermal designers to calculate the equivalent thermal attribute of a compact heat sink without resorting to guesswork, experimentation, or trial. Clearly, the preclusion of iterative operations can provide substantial CPU savings, especially in large-scale heat sink models of populated circuit boards that require coupling between heat sink modules. In view of the current solution being applicable to flat base heat sinks only, the development of closed-form expressions for k_e in other geometric settings will be needed to model commercial heat sinks of diverse shapes.

References

[1]Azar, K., McLeod, R. S., and Caron, R. E., "Narrow Channel Heat Sink for Cooling of High Powered Electronic Components," Eighth IEEE SEMI-THERM Symposium Paper, 1992.

[2]Knight, R. W., Goodling, J. S., and Hall, D. J., "Optimal Design of Forced Convection Heat Sinks – Analytical," *ASME Journal of Electronic Packaging,* Vol. 113, 1991, pp. 313-321.

[3]Knight, R. W., Hall, D. J., Goodling, J. S., and Jaeger, R. C., "Heat Sink Optimization with Application to Microchannels," *IEEE Transactions on Components, Hybrids, and Manufacturing Technology,* Vol. 15, No. 5, 1992, pp. 832-842.

[4]Sasaki, S., and Kishimoto, T., "Optimal Structure for Microgroove Cooling Fin for High Power Lsi Devices," *Electronics Letters,* Vol. 22, No. 25, 1986, pp. 1332-1334.

[5]Lee, S., "Optimum Design and Selection of Heat Sinks," *Eleventh IEEE SEMI-THERM Symposium*, 1995, pp. 48-54.

[6]Patel, C. D., and Belady, C. L., *Modeling and Metrology in High Performance Heat Sink Design*,

Hewlett Packard Laboratories, Palo Alto, California, 1997.

[7]Narasimhan, S., and Majdalani, J., "Characterization of Compact Heat Sink Models in Natural Convection," The ASME International Electronic Packaging Conference and Exhibition Paper 2001-15889, July 8-13, 2001.

[8]Narasimhan, S., and Majdalani, J., "Characterization of Compact Heat Sink Models in Natural Convection," *IEEE Transactions on Components Packaging & Manufacturing Technology –Part A,* Vol. 25, No. 1, 2002, pp. 78-86.

[9]Culham, J. R., Yovanovich, M. M., and Lee, S., "Thermal Modeling of Isothermal Cuboids and Rectangular Heat Sinks Cooled by Natural Convection," *IEEE Transactions on Components Packaging & Manufacturing Technology –Part A,* Vol. 18, No. 3, 1995, pp. 559-566.

[10]Churchill, S. W., and Chu, H. H. S., "Correlating Equations for Laminar and Turbulent Free Convection from a Vertical Plate," *International Journal of Heat and Mass Transfer,* Vol. 18, No. 11, 1975, pp. 1323-1329.

[11]Bejan, A., *Convection Heat Transfer*, 2nd ed., John Wiley, New York, 1982.

[12]Narasimhan, S., and Kusha, B., "Characterization and Verification of Compact Heat Sink Models," *Proceedings of the Heat Transfer and Fluid Mechanics Institute*, 1998, pp. 43-46.

[13]Kusha, B., Rosenblat, S., and Lee, S., Private Communication, Thermal Modeling of Heat Sinks, 2000.